Lab on a Chip

Cancer marker-free enrichment and direct mutation detection in rare cancer cells by combining multi-property isolation and microfluidic concentration

Journal:	*Lab on a Chip*
Manuscript ID	LC-ART-07-2018-000772.R2
Article Type:	Paper
Date Submitted by the Author:	16-Dec-2018
Complete List of Authors:	Kim, Soo Hyeon; Institute of Industrial Science, The University of Tokyo, Ito, Hiroshi; ARKRAY, Inc. Kozuka, Masahiro; ARKRAY, Inc. Takagi, Hidenori ; Arkray Inc Hirai, Mitsuharu; ARKRAY, Inc. Fujii, Teruo; Institute of Industrial Science, University of Tokyo

Cancer marker-free enrichment and direct mutation detection in rare cancer cells by combining multi-property isolation and microfluidic concentration

Soo Hyeon Kim[1,2]*, Hiroshi Ito[3], Masahiro Kozuka[3], Hidenori Takagi[3], Mitsuharu Hirai[3] and Teruo Fujii[1]*

[1]Institute of Industrial Science, The University of Tokyo, Tokyo, JAPAN

[2]JST, PRESTO, Saitama, JAPAN

[3]Research & Development Division, ARKRAY, Inc., Kyoto, JAPAN

Abstract

Genetic analysis, rather than simply counting the number of circulating tumor cells (CTCs), which are rare cancer cells in peripheral blood, has great potential for non-invasive biopsy or "liquid biopsy." However, a practical problem in conventional enrichment of CTCs is that the isolated target cells are mixed with numerous residual leukocytes, and are suspended in a large volume. Hence, further isolation (i.e., cytokeratin (CK)-positive cell picking) or DNA purification is required for downstream genetic analysis after isolation. Here, we propose a novel cancer marker-free method of CTC enrichment by size-based Filtration and Immunomagnetic Negative selection followed by Dielectrophoretic concentration (CTC-FIND) for direct detection of genetic mutations in rare cancer cells suspended in whole blood. A combination of two independent isolation methods based on physical (filtration) and biochemical properties (immunomagnetic negative selection) in CTC-FIND allowed highly efficient cancer marker-free purification (5.1-log depletion of leukocytes). The isolated cells were trapped and concentrated using a microfluidic step-channel device using dielectrophoresis for discrimination and downstream genetic analysis. The feasibility of cancer marker-free enrichment by CTC-FIND was successfully demonstrated by directly detecting mutations in various cancer cells with a very high sensitivity of 1 cell/mL, including EpCAM and CK-negative cells, which were used to spike 8 mL of whole blood. Thus, CTC-FIND can be used with liquid biopsy to detect genetic mutations in wide-ranging CTC subsets, independent of cancer cell-specific marker expression.

Introduction

Circulating tumor cells (CTCs), which are rare cancer cells in peripheral blood, are considered biomarkers that reflect the current disease status of the patient[1]. For instance, the number of CTCs is a strong prognostic factor for overall survival in patients with various cancers, including metastatic breast, colorectal, or prostate cancer[2]. Along with enumeration of cancer cells, their molecular characterization is also important for determining the choice of therapy as CTCs reflect primary tumors and offer insights into the mechanisms of drug resistance[3]. Recent reports on the clinical utilization of CTCs revealed that the genetic properties of CTCs should be investigated, rather than just counting the number of CTCs, using non-invasive biopsy or "liquid biopsy."[4, 5] Extremely low abundance of target cells mixed with a large amount of unwanted cell types (only 1-10 CTCs in a 1 mL blood sample) is the major technical issue in CTC analysis.

Various CTC separation methods utilizing the biochemical and physical properties of target cells have been introduced. The CELLSEARCH® system (the only FDA approved system) is based on biochemical properties and utilizes antibodies immobilized on magnetic beads targeting the epithelial cell adhesion molecule (EpCAM) expressed on the target cancer cell surface. Recently, microfluidic devices for CTC separation have been developed using antibody-coated beads[6] or microstructures[7] targeting EpCAM. However, recent reports on the molecular diversity of CTCs reveal that reliable separation with EpCAM-based positive selection is difficult because of the heterogeneity in EpCAM expression levels in CTCs[8-10]. To address this issue, the concept of negative selection proposed for CTC purification by depletion of leukocytes in blood samples and isolation of target CTCs was successfully demonstrated without labeling the target cells[11, 12]. Different approaches based on the physical properties of target cells have also been widely employed to overcome the presence of EpCAM-negative cells, using dielectrophoresis[13], acoustophoresis[14-16], hydrodynamic force,[17, 18] and microfiltration[19].

For reliable mutation detection, efficient depletion of leukocytes is highly important, because the large amount of DNA from leukocytes reduces the S/N ratio of the target DNA from CTCs. In practice, conventional PCR-based methods for mutation detection require ≥ 1% mutant DNA in the sample[20, 21]. In contrast, positive selection targeting EpCAM, negative selection, or physical property-based separation usually involves difficulties in the efficient removal of leukocytes. With negative selection, numerous residual blood cells still remain in the processed sample because of the large number of leukocytes that need to be selected for depletion. With physical property-based approaches, the overlap of physical properties between cancer cells and leukocytes hinders the achievement of high recovery and purity. A practical problem of negative selection or the physical property-based approach is that isolated target cells are suspended in a

large sample volume. These drawbacks prevent the direct genetic analysis of these cells and an additional laborious isolation process (i.e., cytokeratin (CK)-positive cell picking)[22, 23] or DNA purification process[24, 25] is required for accurate genetic analysis.

Here, we propose a novel method of CTC enrichment by size-based Filtration and Immunomagnetic Negative selection followed by Dielectophoretic concentration (CTC-FIND) that allows for a highly efficient enrichment of rare cancer cells for the direct detection of genetic mutations without target cell labeling. The CTC-FIND system utilizes a combination of physical properties (size-based filtration) and biochemical properties (immunomagnetic negative selection) of cancer cells for purification (Fig. 1). The purified samples are concentrated using a microfluidic device employing dielectrophoresis, and are directly used for genetic analysis. We report the efficiency of each isolation and concentration module using blood samples spiked with cancer cell lines under various experimental conditions. After optimization, molecular characterization of rare cancer cells using the CTC-FIND system was demonstrated by detecting mutations in various cancer cell lines, including EpCAM-positive and -negative cell lines spiked in whole blood.

Results

Concept of CTC-FIND

CTC-FIND consists of highly efficient label-free enrichment and concentration modules for the direct detection of mutations in rare cancer cells from peripheral blood (Fig. 2). First, enrichment of cancer cells was achieved by combining two independent label-free separation methods utilizing the physical and biochemical properties of target cells. Filtration using a slit-shaped microfilter was used to remove blood cells based on their physical properties. Narrow slit-shaped holes and mild filtration conditions were used to efficiently capture even small-sized cancer cells. After collecting the sample trapped on the microfilter, the remaining leukocytes in the sample were further removed using immunomagnetic separation targeting CD45/50 expressed on the leukocyte surface. Next, the purified sample was introduced into the microfluidic device allowing efficient cell trapping by dielectrophoresis (DEP) for the observation of target cells and reduction of the sample volume. The recovered sample from the microfluidic device was directly loaded onto commercially available equipment for mutation detection without further nucleic acid purification processes.

Physical property-based separation: Filtration using slit-shaped microfilter

Target cancer cells in a blood sample were separated based on their physical properties, including size and deformability. Narrow slit-shaped holes (6.5 μm × 88 μm) were developed to efficiently capture the cancer cells. The filter was fabricated with approximately 20,000 slit-shaped holes in a

28 mm^2 area (Fig. 3A). To evaluate the filtration performance, the recovery of cancer cells and nucleated cells was analyzed using various filtration flow rates. Whole blood (8 mL) spiked with the small-sized cancer cell line SW620 (13 μm in diameter) stained with CellTracker Green (approximately 300–400 cells) was loaded onto the reservoir of the filtration device and filtered at a flow rate of 0.1, 1, or 5 mL/min, followed by hemolysis of the residual erythrocytes. Then, the trapped cells, including cancer cells and leukocytes, were stained with Hoechst 33342 (Dojindo) on the microfilter. The stained cells were separated from the microfilter by applying a buffer from the opposite direction, and collected using a micropipette. The collected cells were pipetted into a culture plate and counted after imaging.

The recovery rate, the percentage of the number of collected cells to the number of loaded cells, was calculated for various filtration flow rates (Fig. 3B). At the flow rate of 0.1 mL/min, 100 ± 6% of SW620 cells were recovered and 0.08 ± 0.03% of leukocytes were recovered. Since the deformability of leukocytes is bigger than that of cancer cells[26], small-sized cancer cells could be separated efficiently with the present slit-shaped microfilter. With an increased flow rate of 1 mL/min, 106 ± 12% of SW620 cells were recovered, while only 0.03 ± 0.03% of leukocytes were recovered. However, when the flow rate was further increased to 5 mL/min, the recovery of SW620 cells and leukocytes was decreased to 73 ± 13% and 0.01 ± 0.0005%, respectively, since the target cells and leucocytes passed through the microfilter without being trapped due to the increased shear stress. These results indicate that the present slit-shaped microfilter shows efficient capture of target cancer cells from blood at a flow rate of 1 mL/min. No clogging of the filtration module was observed with the present large hole-to-surface ratio (41%) of the microfilter at a flow rate of 0.1, 1 and 5 mL/min, thus allowing high throughput filtration. Moreover, the high hole-to-surface ratio allows for the direct use of the whole blood without dilution.

To evaluate the separation performance on the cancer cells having high deformability, recovery of keratin-free cells, having 60% higher cell deformability[27], was investigated with the filtration module. SNU-1 cells (CK negative; 17 μm in diameter) were spiked into 8 mL of whole blood and filtered at a flow rate of 1 mL/min. The recovery of SNU-1 cells was 79 ± 14%. Although the recovery of SNU-1 cells was slightly decreased compared to that of SW620 cells due to the high deformability of the former, the filtration module can be used for the efficient separation of keratin-free cells.

Biological property-based separation: Immunomagnetic depletion

Purification based on the biochemical properties of leukocytes was carried out using immunomagnetic depletion of CD45/50+ cells. The conventional microfluidic device that enables

magnetophoresis showed a good performance for the separation of magnetic bead-labeled unwanted cells from the sample[12]. However, the requirement of precise control of carrier flow by multiple pumps in a microfluidic channel needs to be addressed. Meanwhile, the conventional method using microcentrifuge tubes prevents efficient separation of magnetic bead-labeled cells because the cells need be moved for a long distance in the tube. For efficient magnetic separation, a simple method utilizing a thin tubing and a neodymium bar magnet was proposed in order to increase the interaction between the magnetic field and cells, by placing the bar magnet besides the tubing to attract leukocytes labeled with magnetic beads (Fig. 4A and 4B). The cells labeled with magnetic beads were attracted to the side surface of the tubing and the target cells without labeling were settled down to the bottom surface of the tubing by gravity. Since the direction of target cell attraction was perpendicular to that of unwanted cell attraction, target cells could be efficiently separated from the unwanted cell types labeled by magnetic beads. Moreover, a liquid/gas interface was used to sweep away the target cells settled on the bottom surface of the tubing by pushing air into the tubing for efficient collection of target cells.

To investigate the purification efficiency of the present method utilizing magnetic depletion, SW620 cells were separated from leukocytes. A mixture containing a small number of SW620 cells stained with CellTracker Green and leukocytes labeled with magnetic beads together with Alexa 594-antibody conjugates was introduced into the thin tubing, and separated using the bar magnet for 15 min after stopping the flow. The settled cancer cells were collected using the liquid/gas interface with various air-flow rates of 25, 100, and 500 μL/min. Figure 4C shows the recovery for both SW620 cells and leukocytes with respect to the flow rates of the air syringe. For the low flow rate of 25 μL/min, the recovery of SW620 was low, at 62 ± 17%. The large standard deviation is because the drag force induced by the interface was not enough to sweep out the settled target cells. However, for the high flow rate of 500 μL/min, the recovery of SW620 cells was very high (89 ± 3%) but the recovery of leukocytes was also increased because the strong drag force by the interface flushed the magnetically trapped leukocyte cells. Hence, a moderate flow rate of 100 μL/min showed good performance for the recovery of SW620 cells (85 ± 3%) and depletion of leukocytes (99.8 ± 0.1%).

The advancing liquid/gas interface allows for efficient collection of target cells from the thin tubing. Since the target cells were settled at the bottom of the tubing, the low velocity around the surface of the tubing prevented the efficient collection of settled cells. Without the interface, only 10% of settled target cells were collected at the outlet of the channel. When the interface was formed in the channel, the advancing interface physically pushed the cells out of the tubing. Hence, the liquid/gas interface allows collection of highly purified cells from the outlet of the tubing.

Cell trapping and concentration using a dielectrophoretic microfluidic device

The present multi-separation method efficiently removes unwanted cell types. However, the enriched target cells were suspended in a relatively large volume (0.6 mL). The sample volume needs to be reduced for genetic analysis and the target cells observed on a substrate to enable discrimination. The conventional centrifugation and sample transfer process increases the risk of critical loss with such a small number of cells (less than 500 cells in 0.6 mL). To overcome the risk of cell loss, a microfluidic device utilizing DEP was implemented for the observation and concentration of cells suspended in a large sample volume after purification (Fig. 5A). The microfluidic device allows for efficient DEP trapping by drastically decreasing the flow velocity around cells with a sharply expanded channel height[28]. Figure 5B shows a representative image of trapped SW620 cells in the microfluidic device.

The feasibility of the microfluidic device was demonstrated by trapping and collecting a mixture of fixed SW620 cells and leukocytes. The cells were suspended in PBS containing 1% paraformaldehyde and fixed for 15 min at room temperature. After washing with PBS, a mixture of 102 ± 10 SW620 cells and 103 ± 16 leukocytes suspended in 1 mL of a low-conductivity buffer (10 mM HEPES, 0.1 mM $CaCl_2$, 59 mM D-glucose, 236 mM sucrose, and 0.2% w/v BSA) was introduced into the device and trapped using DEP by applying an electrical potential of 20 Vpp at 1 MHz. The trapped cells were collected from the inlet by injecting an additional 20 μL of reagent to the outlet of the device, where 100 ± 10 SW620 cells and 98 ± 7 leukocytes were collected from the device with high recovery rates of 98% and 95% for SW620 cells and leukocytes, respectively. The collected cells were resuspended in 20 μL, indicating that the cells were concentrated 50-fold (Fig. 5C). The small volume of the microfluidic device (10 μL in total) allows for efficient observation and concentration of cells suspended in a large sample volume.

Purification and concentration of rare cancer cells using the integrated CTC-FIND method

To evaluate the CTC purification and concentration performance using CTC-FIND, 1,000 SW620 cells (stained with CellTracker Green) spiked in 8 mL of whole blood were filtered, negatively selected, and trapped with DEP. Six hours were required for the whole CTC-FIND process. A sample (200 μL) after each step was collected for calculating the recovery, purification factor, defined as the ratio of cancer cell purity to the initial purity, and concentration factor, defined as the ratio of cancer cell concentration to the initial concentration. Figure 6A shows recovery of SW620 cells after each step. The recovery was decreased after the filtration step because of cell loss during the cell collection process from the microfilter, and the final recovery of cancer cell

was 42 ± 9%. The final purity of cancer cells to the leukocytes was 54 ± 6%. No erythrocyte remained in the processed sample. Figure 6B shows the changes in the purification and concentration factors during the CTC-FIND process. The purification factor was drastically increased (7.3×10^3 times) after filtration, and was further increased (2.6×10^4 times) after immunomagnetic negative selection. Only 350 ± 87 leukocytes remained after the CTC-FIND process and log depletion of leukocytes (calculated from logarithm of the number of initial leukocytes divided by the number of remaining leukocytes to base 10) was 5.1 ± 0.2. Moreover, the purified sample was resuspended in a small volume (20 μL) of reagent, and the concentration factor was increased to 1.7×10^2 times. These features allow for direct analysis of the treated sample without laborious target cell selection and centrifugation.

Mutation detection using the CTC-FIND method

The feasibility of the integrated method was demonstrated by detecting the genetic mutations of the cancer cells spiked in 8 mL of whole blood after their enrichment using CTC-FIND. A very small number (6–12 cells) of various cancer cells including NCI-H1650, NCI-H1975, or A549 cells were spiked into 8 mL of whole blood. The whole blood samples were directly filtered, washed, and fixed on the microfilter. For the discrimination of cancer cells, FITC labeled anti-CK antibodies were loaded onto the microfilter. For the staining and magnetic labeling of leukocytes, cocktails of mouse anti-CD45 and CD50 antibodies, and secondary antibody cocktails of anti-mouse antibodies labeled with biotin and Alexa 594, containing Hoechst 33342, and magnetic beads coated with neutralized avidin were sequentially loaded on the microfilter. The cells were further purified, concentrated, and imaged with the CTC-FIND method. The recovered cells suspended in 20 μL volume were directly loaded onto a commercialized genetic analysis system (i-densy™, ARKRAY Inc., Japan) and the mutations in each cell line were detected by monitoring the dissociation temperature of quenching probes (QPs) after PCR amplification. The EGFR ex19del in NCI-H1650 cells was detected with a high sensitivity of 1 cell/mL (8 cancer cells spiked in 8 mL of whole blood, Supplementary Table 2). Additionally, the EGFR L858R mutation in NCI-H1975 cells was also successfully detected with a very high sensitivity of 0.875 cell/mL. No mutation was detected from the sample of A549 cells (wild type).

Moreover, robust mutation detection independent of the conventionally used CTC markers EpCAM or CK was demonstrated by detecting the KRAS mutation in SNU-1 (EpCAM negative and CK negative), SW620, or MCF-7 cells spiked in 8 mL of whole blood, where SNU-1 cells were stained with a fluorescent dye (CellTracker Orange) before the spike-in experiment for discrimination. The KRAS mutation was successfully detected in SW620 and SNU-1 (KRAS

mutation positive cell lines) spiked samples, whereas no mutation was detected in the MCF-7 (wild-type) spiked sample as summarized in Table 1. The KRAS mutation was successfully detected with the present system in SNU-1 cells even though they were not stained with CK antibodies. The recovery of cancer cells was 44 ± 24% (calculated from the data of Supplementary Table 2 and Table 1). The results indicate that the cancer marker-free CTC-FIND method allows efficient and robust enrichment of CTCs from whole blood followed by detection of mutations independently of cancer cell markers.

Table 1 Performance of CTC-FIND method in mutation detection from various cancer cell lines spiked in 8 mL of whole blood

Spiked cell line	KRAS mutation	Expected count (cells/8 mL)	Detection		
			Cancer cell count (cells)	Remained leukocyte count (cells)	KRAS codon 12/13
SW620	KRAS G12V	8 (SD±2)	6	48	Positive
SNU-1	KRAS G12D	12 (SD±4)	0 (4)*	154	Positive
MCF-7	Wild type	15 (SD±5)	13	164	Negative

*SNU-1 cells were stained with a fluorescent dye (CellTracker Orange) before the spike-in experiment for discrimination.

Discussion

We have shown that the CTC-FIND method allows for highly efficient cancer marker-free enrichment of CTCs suspended in whole blood, followed by mutation detection in cancer cells. The technical difficulties of low target cell purity in detecting mutations from rare cancer cells were efficiently eliminated using two independent cancer marker-free separation methods based on the physical and biochemical properties of target cancer cells and leukocytes. Moreover, the use of a concentration device allowed for the resuspension of target cells into a significantly reduced volume of reagent for genetic analysis, and eliminated the risk of critical loss of rare cancer cells. The highly purified and concentrated sample obtained with the CTC-FIND method allows for direct loading of the processed sample onto the equipment used for downstream analysis. This unique feature of the present CTC-FIND was successfully demonstrated by detecting heterogeneous phenotypes, such as EpCAM or CK negative cancer cells based on their genomic mutations.

Recently, physical property-based isolation methods have been widely implemented in microfluidic devices to address an EpCAM-negative issue. However, the critical problem with this method is that the physical properties of target cells overlap with those of unwanted leukocytes. For instance, small-size CTCs were observed in a blood sample from a patient[29]. This indicates that achieving both high recovery and purity is difficult with physical property-based methods. In the present study, narrow slit-shaped holes and a moderate filtration velocity was used to capture small-sized cancer cells, and the practical issue of residual leukocytes was overcome by integrating a biochemical property-based negative selection method to complement the physical property-based method.

Meanwhile, biological property-based leukocyte depletion methods that involve the removal of magnetic bead-labeled leukocytes from the blood sample have been proposed. Although the depletion methods showed robust separation of various cancer cells from the sample, the practical problem of leukocyte depletion is the low purity of the processed sample. It is thus difficult to efficiently remove the large number of leukocytes from a sample. The negative selection method proposed by the Toner group showed a 2.5-log depletion of leukocytes by using magnetic beads[12]. The final discrimination or selection relied on protein makers such as EpCAM or CK, even though the separation was carried out without labeling. Direct genetic analysis was not carried out because the large amounts of remaining leukocytes mixed with target cells and the large volume of treated samples could prevent reliable downstream analysis. The CTC-FIND however, showed a 5.1-log depletion of leukocytes, indicating that only several hundred leukocytes remained when 8 mL of whole blood was processed, and the cells were resuspended in 20 μL volume of reagent for analysis. Although the recovery of cancer cells (44 $\pm$ 24%) was not as high as that reported by previous methods, the high purity of the cancer cells obtained allows for a sensitive detection of mutated DNA in cancer cells.

In the present study, practical improvements on both filtration and immunomagnetic separation were achieved by implementing a slit-shaped microfilter for a large hole-to-surface ratio, and thin tubing with a bar magnet for enhanced interaction between magnetic beads and the magnet, respectively. Although our previous oval microfilter showed good performance in CTC separation[19], the throughput was not sufficient for a large sample volume because the low hole-to-surface ratio (19%) and small total area of holes (3.7 mm^2) caused increase of velocity when the cell bodies clogs the holes on the microfilter. To overcome this drawback, slit-shaped holes, with a high hole-to-surface ratio (41%) and large total area of holes (11 mm^2), were used to prevent significant increase of flow velocity by the trapped cell bodies. In the present setup, approximately 20% of holes were clogged by the cell bodies when 1.4×10^4-leukocytes were trapped on the microfilter

(70% for previous oval microfilter). Such high hole-to-surface ratio and area of holes of the microfilter shows good performance on the filtration. Further increased hole-to-surface ratio would increase the throughput but it would also increase the risk of breakage of the filter. Another practical improvement was achieved by using a thin tubing and bar magnet for immunomagnetic separation. The conventional method using microcentrifuge tubes prevents efficient separation of magnetic bead-labeled cells because the target cells move for long distances in the tube. On the other hand, microfluidic devices enabling magnetophoresis showed low throughput and requirement of precise control of carrier flow in the channel. In the present immunomagnetic negative selection module, the thin tubing and bar magnet were used to increase interaction between the magnet and magnetic beads. A small inner diameter (3.1 mm) of the thin tubing facilitates migration of magnetic bead-labeled cells by decreasing the travel distance and a large surface to volume ratio of the thin tubing allows for efficient immobilization of large amounts of unwanted leukocytes. Moreover, the advancing liquid/gas interface used for the collection of target cells allowed for an efficient collection of target cells settled at the bottom of the tubing. No precise control of flow is required to operate the module. By combining these two improved methods, the target cancer cells were separated from whole blood with very high purity.

The order in which each module is carried out is important for efficient separation. Since immunomagnetic depletion cannot remove erythrocytes from the blood sample, filtration should be carried out prior to immunomagnetic depletion. Moreover, leukocyte labeling on the microfilter allowed rapid reagent changes without centrifugation. Hence, the present order of separation, filtration, followed by immunomagnetic separation, allows for efficient separation.

Although the concept of CTC-FIND was successfully demonstrated here, additional optimization is required to build an automated CTC analysis system. Each process should be integrated into a single system and the sample transfer process should be automated. A manual sample transfer process between each component could introduce experimental errors when performed by untrained individuals. Since the filtered cells should be collected from the filtration module and transferred to the immunomagnetic negative selection module, automated pipetting system is required to connect the interface of filtration and negative selection module. Meanwhile, the outlet of the negative selection module can be directly connected to the inlet of the microfluidic device for DEP trapping. In this case, the operating flow rate of the microfluidic device should be increased up to 100 μL/min by optimizing experimental parameters to use the same operation flow rate that is used for the immunomagnetic negative selection module. Moreover, the time required for the total process could be further shortened by optimizing the experimental parameters.

The circulating tumor DNA (ctDNA) in peripheral blood is an emerging biomarker for the non-invasive tumor genotyping by detecting mutations. Although ctDNA testing has high diagnostic sensitivity and specificity, it is difficult to be an alternative to CTC testing because ctDNA and CTC have different nature and are released from different stages. Rather, ctDNAs and CTCs provide complementary information on the tumor genotyping and improve the reliability of liquid biopsy by using them together[24]. We believe that our robust method will facilitate highly sensitive CTC testing and can be used together with sensitive ctDNA testing to determine reliable liquid biopsy for therapeutic target selection, and monitoring response and resistance to treatment.

Conclusions

We successfully demonstrated that the CTC-FIND method allows direct detection of mutations in rare cancer cells with a very high sensitivity of 1 cancer cell/mL of whole blood. By combining two independent label-free separation methods of size-based filtration followed by immunomagnetic leukocyte depletion, highly purified rare cancer cells were obtained (with 5.1-log depletion of leukocytes). Moreover, by employing a microfluidic device for concentrating the purified sample, mutations in rare cancer cells were directly detected without relying on cancer cell marker proteins. These unique features of the present system would be beneficial for addressing critical issues of CTC analysis, including heterogeneity of protein markers on CTCs. We believe that our novel method will be useful for genetic analysis in wide-ranging CTC subsets, independent of the expression of specific antigens, and may be particularly effective for CTCs that have changed their phenotype. By monitoring genetic mutations rather than simply counting the number of CTCs, drug resistance mutations could be detected without the requirement of biopsy samples. To further assess the feasibility of this system, we plan to integrate the individual components into a single system for an automated CTC analysis system.

Material and methods

Cell culture and sample preparation

The human lung cancer cell lines (NCI-H1975 and NCI-H1650) and gastric cancer cell line (SNU-1) were obtained from the American Type Culture Collection (ATCC). The colorectal cancer cell line (SW620) and breast cancer cell line (MCF-7) were obtained from the European Collection of Authenticated Cell Cultures (ECACC). SW620 was cultured in a humidified incubator at 37 °C and the other cell lines were cultured in a humidified incubator at 37 °C in an atmosphere of 5% CO_2. The culture media were RPMI 1640 (Thermo Fisher Scientific, USA) for NCI-H1975, NCI-H1650

and SNU-1, L-15 (Thermo Fisher Scientific, USA) for SW620, and MEM alpha (Thermo Fisher Scientific, USA) for MCF-7. The base media were supplemented with fetal bovine serum (10%; Sigma-Aldrich, USA) and a penicillin-streptomycin solution (1%; Thermo Fisher Scientific, USA). The mean diameter of each cell line (NCI-H1975: 18 μm; NCI-H1650: 18 μm; SNU-1: 17 μm; SW620: 13 μm; MCF-7: 19 μm) was measured by using a cell counter (Moxi Z; Orflo Technologies, USA). The suspended cancer cells were spherical.

Fluorescence-labeled and unlabeled cells were used for spike-in experiments. To prepare fluorescence-labeled cells, harvested cells were stained with CellTracker Green CMFDA or Orange CMRA (Life Technologies, USA). To count the number of spiked cells, the same volume of cell suspension used for the spike-in experiments was pipetted into each well of a 384-well plate and the images of each well were taken using a fluorescence microscope (IX 73; Olympus, Japan) with a digital CCD camera (DS-Qi1Mc; Nikon, Japan). The number of spiked cells was calculated from the average over three replicates. On the other hand, the number of unlabeled cells pipetted into the well was counted after staining the cells using Calcein AM (Dojindo, Japan).

Blood samples were collected from healthy volunteers into evacuated blood collection tubes with EDTA-2K (Terumo co., Japan). Leukocytes were separated from healthy donor blood samples using separation kits (HetaSep from Stemcell Technologies, Canada). All experiments involving blood samples were performed in compliance with the relevant laws and institutional guidelines of Japan and approved by the institutional committee at ARKRAY, Inc. All healthy volunteers provided informed consent for blood samples to be collected.

The purity of cancer cells was calculated from the number of cancer cells divided by the number of total cells in a sample.

Construction of filtration module and filtration

The microfilter for cancer cell separation was fabricated by nickel electroformation (Optnics Precision Co. Ltd., Japan). The microfilter had slit-shaped holes (6.5 × 88 μm) with a hole-to-surface ratio of 41%. The filtration module was constructed by sandwiching the microfilter between the sample reservoir and the outlet connected to a tube pump using two doughnut-shaped double-stick tapes. The diameter of the filtration area was 6 mm, where about 20,000 holes were placed. The sample was loaded onto the reservoir of the filtration module and filtered by the tube pump connected to the module outlet. After washing with phosphate buffed saline containing EDTA (PBS-EDTA), ammonium chloride solution (0.08%) was loaded for the hemolysis of remained erythrocytes at the edge of the filtration module.

Staining and magnetic labeling of leukocytes on the microfilter

For the labeling of leukocytes on the microfilter, PBS containing 0.2% bovine serum albumin (PBS-BSA) with the addition of goat serum (Wako Pure Chemical Industries, Ltd, Japan) and avidin (Santa Cruz Biotechnology, TX, U.S.A) was loaded on the microfilter to prevent nonspecific binding. After incubation within 10 min and washing with PBS, the cells were labeled with anti-human CD45 antibody (clone: HI30; Affymetrix, USA) and anti-human CD50 antibody (Affymetrix) in the PBS-BSA containing the goat serum and biotin (Tokyo Chemical Industry Co., Ltd, Japan) within 15 min, followed by washing with PBS. Then, the cells were labeled with a cocktail of secondary antibodies composed of rabbit anti-mouse IgG (F(ab')2 specific) goat antibody labeled with Alexa 594 (Jackson ImmunoResearch, USA) and anti-mouse IgG (Fc specific) goat antibody labeled with biotin (Sigma-Aldrich, MO, U.S.A) in the PBS-BSA containing Hoechst33342 and goat serum within 15 min. After washing with PBS, the cells were mixed with neutralized avidin-coated magnetic beads (25 μg, Bio-Adembeads StreptaDivin, 300 nm, Ademtech SA, France) within 30 min.

Immunomagnetic depletion

A sample was loaded into a thin tubing (polyvinyl chloride tube for the infusion pump, inner diameter 3.1 mm; Terumo) through a sample inlet on the three-way valve, where the total sample volume was 1 mL. The neodymium bar magnet (200 × 15 × 5 mm; NeoMag Co., Ltd., Japan) was attached to the side of the tubing to attract leukocytes labeled with magnetic beads. The magnetic bead-labeled cells were attracted to the magnet for 15 min without flow. To collect the target cancer cells using a liquid/gas interface, air was introduced into the tubing by pushing a syringe filled with air after changing the direction of the three-way valve. The solution containing target cells was then collected at the sample outlet.

Fabrication of a microfluidic device for concentration

The microfluidic device consists of a glass substrate containing an indium tin oxide (ITO) electrode and a polydimethylsiloxane (PDMS) fluidic channel, whose fabrication process is described in detail elsewhere[28]. In brief, to fabricate the ITO electrodes, an ITO coated glass substrate (GEOMATEC co., Japan) coated with a positive-type photoresist (S1813; Shipley far Ltd., USA) was exposed to ultraviolet light through a photo-mask for the electrode, followed by development and rinsing using a developer (AZ developer; AZ Electronic Materials) and deionized water. After photolithography, the substrate was dipped into an etchant (ITO-02; Kanto Kagaku Co., Japan) for

5 min at 40 °C. The substrate was cleaned with acetone to remove the photoresist layer and was rinsed with isopropyl alcohol.

The PDMS microfluidic channel was fabricated using a standard replica molding process. A negative-type photoresist (SU-8 3035, MicroChem Co., USA) was coated on a silicon wafer. After soft baking (95 °C for 15 min), the resist was exposed to ultraviolet light through a photo-mask patterned for the thin fluidic channel and baked at 95 °C for 5 min, followed by development and rinsing using an SU-8 developer and isopropyl alcohol, respectively. Additional negative-type photoresist (SU-8 2100; MicroChem Co., USA) was coated on the silicon wafer to form a thick fluidic channel. The substrate was then soft baked and exposed to ultraviolet light through a photo mask for the thick channel after alignment with the thin fluidic channel. After development and rinsing, a prepolymer of PDMS mixed with a curing reagent (10:1 mass ratio) was poured over the fluidic channel mold master. Polymerized PDMS was then peeled off from the mold master and holes were punched out using a 1 mm biopsy punch. The PDMS fluidic channel was bonded with the ITO electrode substrate after exposure to O_2 plasma using a reactive ion etching machine (RIE-10NR, Samco Co., Japan).

The fabricated device is composed of a glass substrate having interdigitated electrodes with 40 μm lines and 60 μm spaces, and a PDMS microfluidic channel that has a sharply expanded channel height from 50 to 100 μm. The microfluidic channel has a hexagonal observed area whose distance from inlet to outlet is 10 mm and the maximum width is 7 mm.

Cell trapping using the microfluidic device

The microfluidic device was placed on an x-y translational stage located on an inverted microscope (IX 73; Olympus, Japan). The cells were delivered into the microfluidic device at 20 μL/min by withdrawing a syringe connected to the outlet of the microfluidic device using a syringe pump (YSP-201; YMC Co., Ltd., Japan). The cells were trapped at the edge of the electrodes by applying a sinusoidal electric potential (peak-to-peak voltage of 20 V at 1 MHz) to the ITO electrodes using a function generator (WF1973; NF Corp., Japan). The trapped cells in the device were monitored with a digital CCD camera (DS-Qi1Mc; Nikon, Japan, Japan) installed on the microscope.

Mutation detection

The genetic mutations of cancer cell lines spiked in blood were detected without nucleic acid purification. After enrichment of CTCs using CTC-FIND, trapped cells were recovered from the inlet of the microfluidic device by loading 20 μL of reagents containing Proteinase K and the surfactant Nonidet™ P-40 to the outlet, and the complete recovered samples were directly loaded

onto a commercialized genetic analysis system (i-densy™, Arkray Inc., Japan). After amplification of target sequences by PCR, the presence of genetic mutations in the amplified sequences was detected by monitoring the dissociation temperature of quenching probes (QPs) (Nippon Steel & Sumikin Echo-Tech Corporation, Japan). EGFR L858R (NCI-H1975), EGFR ex19del (NCI-H1650), and KRAS (SW620 and SNU-1) mutations were tested using the detection conditions (primer sets, QPs, and PCR conditions) indicated in Supplementary Table 1.

Acknowledgements

This research was supported by JST, PRESTO Grant Number JPMJPR17H3, Japan.

Contact

* S. H. Kim, Tel: +81-3-5452-6213; shkim@iis.u-tokyo.ac.jp
T. Fujii, Tel: +81-3-5452-6211; tfujii@iis.u-tokyo.ac.jp

References

1. G. Attard, J. F. Swennenhuis, D. Olmos, A. H. Reid, E. Vickers, R. A'Hern, R. Levink, F. Coumans, J. Moreira, R. Riisnaes, N. B. Oommen, G. Hawche, C. Jameson, E. Thompson, R. Sipkema, C. P. Carden, C. Parker, D. Dearnaley, S. B. Kaye, C. S. Cooper, A. Molina, M. E. Cox, L. W. Terstappen and J. S. de Bono, *Cancer Res*, 2009, 69, 2912-2918.
2. M. C. Miller, G. V. Doyle and L. W. Terstappen, *J Oncol*, 2010, 2010, 617421.
3. C. Alix-Panabieres and K. Pantel, *Clin Chem*, 2013, 59, 110-118.
4. M. Yu, S. Stott, M. Toner, S. Maheswaran and D. A. Haber, *J Cell Biol*, 2011, 192, 373-382.
5. J. Zhang, K. Chen and Z. H. Fan, *Adv Clin Chem*, 2016, 75, 1-31.
6. S. Kim, S. I. Han, M. J. Park, C. W. Jeon, Y. D. Joo, I. H. Choi and K. H. Han, *Anal Chem*, 2013, 85, 2779-2786.
7. S. Nagrath, L. V. Sequist, S. Maheswaran, D. W. Bell, D. Irimia, L. Ulkus, M. R. Smith, E. L. Kwak, S. Digumarthy, A. Muzikansky, P. Ryan, U. J. Balis, R. G. Tompkins, D. A. Haber and M. Toner, *Nature*, 2007, 450, 1235-1239.
8. A. van de Stolpe, K. Pantel, S. Sleijfer, L. W. Terstappen and J. M. den Toonder, *Cancer Res*, 2011, 71, 5955-5960.
9. T. M. Gorges, I. Tinhofer, M. Drosch, L. Rose, T. M. Zollner, T. Krahn and O. von Ahsen, *BMC Cancer*, 2012, 12, 178.

10. A. Vila, M. Abal, L. Muinelo-Romay, C. Rodriguez-Abreu, J. Rivas, R. Lopez-Lopez and C. Costa, *PloS One*, 2016, 11, e0163705.
11. N. M. Karabacak, P. S. Spuhler, F. Fachin, E. J. Lim, V. Pai, E. Ozkumur, J. M. Martel, N. Kojic, K. Smith, P. I. Chen, J. Yang, H. Hwang, B. Morgan, J. Trautwein, T. A. Barber, S. L. Stott, S. Maheswaran, R. Kapur, D. A. Haber and M. Toner, *Nat Protoc*, 2014, 9, 694-710.
12. E. Ozkumur, A. M. Shah, J. C. Ciciliano, B. L. Emmink, D. T. Miyamoto, E. Brachtel, M. Yu, P. I. Chen, B. Morgan, J. Trautwein, A. Kimura, S. Sengupta, S. L. Stott, N. M. Karabacak, T. A. Barber, J. R. Walsh, K. Smith, P. S. Spuhler, J. P. Sullivan, R. J. Lee, D. T. Ting, X. Luo, A. T. Shaw, A. Bardia, L. V. Sequist, D. N. Louis, S. Maheswaran, R. Kapur, D. A. Haber and M. Toner, *Sci Transl Med*, 2013, 5, 179ra147.
13. S. Shim, K. Stemke-Hale, A. M. Tsimberidou, J. Noshari, T. E. Anderson and P. R. Gascoyne, *Biomicrofluidics*, 2013, 7, 11807.
14. M. Antfolk, C. Magnusson, P. Augustsson, H. Lilja and T. Laurell, *Anal Chem*, 2015, 87, 9322-9328.
15. M. Antfolk, C. Antfolk, H. Lilja, T. Laurell and P. Augustsson, *Lab Chip*, 2015, 15, 2102-2109.
16. P. Li, Z. Mao, Z. Peng, L. Zhou, Y. Chen, P. H. Huang, C. I. Truica, J. J. Drabick, W. S. El-Deiry, M. Dao, S. Suresh and T. J. Huang, *Proc Natl Acad Sci U S A*, 2015, 112, 4970-4975.
17. E. Sollier, D. E. Go, J. Che, D. R. Gossett, S. O'Byrne, W. M. Weaver, N. Kummer, M. Rettig, J. Goldman, N. Nickols, S. McCloskey, R. P. Kulkarni and D. Di Carlo, *Lab Chip*, 2014, 14, 63-77.
18. H. W. Hou, M. E. Warkiani, B. L. Khoo, Z. R. Li, R. A. Soo, D. S. Tan, W. T. Lim, J. Han, A. A. Bhagat and C. T. Lim, *Sci Rep*, 2013, 3, 1259.
19. S. Matsusaka, M. Kozuka, H. Takagi, H. Ito, S. Minowa, M. Hirai and K. Hatake, *Cancer Lett*, 2014, 355, 113-120.
20. W. Pao and M. Ladanyi, *Clin Cancer Res*, 2007, 13, 4954-4955.
21. K. Goto, M. Satouchi, G. Ishii, K. Nishio, K. Hagiwara, T. Mitsudomi, J. Whiteley, E. Donald, R. McCormack and T. Todo, *Ann Oncol*, 2012, 23, 2914-2919.
22. A. Morimoto, T. Mogami, M. Watanabe, K. Iijima, Y. Akiyama, K. Katayama, T. Futami, N. Yamamoto, T. Sawada, F. Koizumi and Y. Koh, *PLoS One*, 2015, 10, e0130418.
23. T. Masuda, W. Song, H. Nakanishi, W. Lei, A. M. Noor and F. Arai, *PLoS One*, 2017, 12, e0174937.

24. T. K. Sundaresan, L. V. Sequist, J. V. Heymach, G. J. Riely, P. A. Janne, W. H. Koch, J. P. Sullivan, D. B. Fox, R. Maher, A. Muzikansky, A. Webb, H. T. Tran, U. Giri, M. Fleisher, H. A. Yu, W. Wei, B. E. Johnson, T. A. Barber, J. R. Walsh, J. A. Engelman, S. L. Stott, R. Kapur, S. Maheswaran, M. Toner and D. A. Haber, *Clin Cancer Res*, 2016, 22, 1103-1110.

25. E. Kidess-Sigal, H. E. Liu, M. M. Triboulet, J. Che, V. C. Ramani, B. C. Visser, G. A. Poultsides, T. A. Longacre, A. Marziali, V. Vysotskaia, M. Wiggin, K. Heirich, V. Hanft, U. Keilholz, I. Tinhofer, J. A. Norton, M. Lee, E. Sollier-Christen and S. S. Jeffrey, *Oncotarget*, 2016, 7, 85349-85364.

26. M. M. Ferreira, V. C. Ramani and S. S. Jeffrey, *Mol Oncol*, 2016, 10, 374-394.

27. K. Seltmann, A. W. Fritsch, J. A. Kas and T. M. Magin, *Proc Natl Acad Sci U S A*, 2013, 110, 18507-18512.

28. S. H. Kim, H. Ito, M. Kozuka, M. Hirai and T. Fujii, *Biomicrofluidics*, 2017, 11.

29. F. A. Coumans, G. van Dalum, M. Beck and L. W. Terstappen, *PLoS One*, 2013, 8, e61770.

Figure Legends

Figure 1 Multi-property isolation.

Physical and biological properties are used for cancer marker-free isolation of rare cancer cells from blood samples. Size-based filtration with a slit-shaped microfilter is used to remove erythrocytes and small-sized leukocytes. The significantly reduced residual leukocytes are further depleted using magnetic beads targeting CD45/50.

Figure 2 A schematic illustration of CTC-FIND.

Whole blood samples are directly used for rare cell analysis without dilution. The target cells are isolated by using the multi-property isolation method utilizing filtration and immunomagnetic depletion, and purified cells are then trapped into the microfluidic device using dielectrophoresis for concentration and discrimination of target cells. The concentrated samples are directly loaded to an equipment for mutation detection. This method allows highly efficient purification and concentration of cancer cells directly from whole blood.

Figure 3 Size-based filtration module.

A) Images of the filtration module. Slit-shaped holes were used to increase the hole-to-surface ratio, where the size of hole was 6.5 μm × 88 μm and the hole-to-surface ratio was 41%. A microfilter was immobilized in the reservoir for sample loading using double-stick tape. Scale bar is 50 μm. B) Recovery of SW620 cells and leukocytes as a function of flow rate. SW620 cells were spiked into whole blood and the number of cells remaining on the microfilter was counted after collection.

Figure 4 Immunomagnetic negative selection module.

A) A schematic illustration of the immunomagnetic negative selection module. Magnetic bead-labeled leukocyte cells are introduced into a thin tubing. A bar magnet is placed beside the tubing resulting in leukocyte attraction to the magnet. The target cancer cells are settled by gravity. The settled target cells are collected by using an advancing gas-liquid interface induced by flowing air into the tubing. B) An experimental setup of the immunomagnetic negative selection module. A thin tubing was connected with a three-way valve, and the bar magnet was placed beside the tubing. C) Recovery of SW620 cells and leukocytes as a function of the air flow rate. SW620 cells were mixed with magnetic bead-labeled leukocytes and collected after negative selection. The number of SW620 cells and leukocytes was counted after collection.

Figure 5 Localization and concentration of cells using a microfluidic step-channel.

A) Schematic illustration of cell trapping and collection. Cells suspended in a buffer are introduced into the microfluidic device with a sharply expanded step. The cells are attracted to the high electric field regions and trapped at the edge of electrodes using DEP. Since the flow velocity around the cells is rapidly decreased behind the step, the cells are trapped at the electrodes. The trapped cells are imaged and collected from the inlet by injecting an additional 20 μL solution to the outlet of the device. B) Fluorescence and bright field image of the device after cancer cell trapping. The scale bar is 100 μm. C) Concentration of cells before loading and after collection. Since the volume of the microfluidic device was 10 μL, the cells were collected in a small volume (20 μL) of reagent.

Figure 6 Changes in recovery, purification and concentration factors.

For evaluating the system, 1,000 SW620 cells spiked in 8 mL of whole blood were filtered, negatively selected, and trapped using the CTC-FIND method. The concentration of leukocytes in the blood samples was $6.1 \pm 1.8 \times 10^6$ cells/mL. A) Recovery of cancer cells after each step. Error bars are plotted as the standard deviation over three replicates. B) Purification and concentration factors after each step. The purification factor was drastically increased after filtration and negative selection, whereas the concentration factor was increased after DEP trapping. Error bars are plotted as the standard deviation over three replicates.

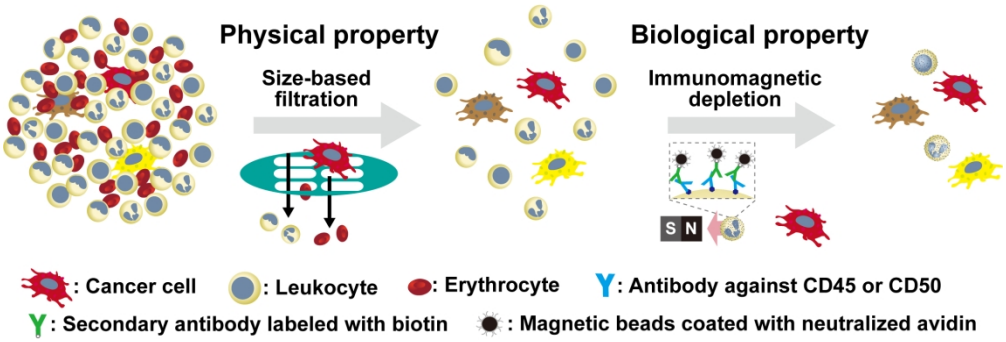

Figure 1 Multi-property isolation.

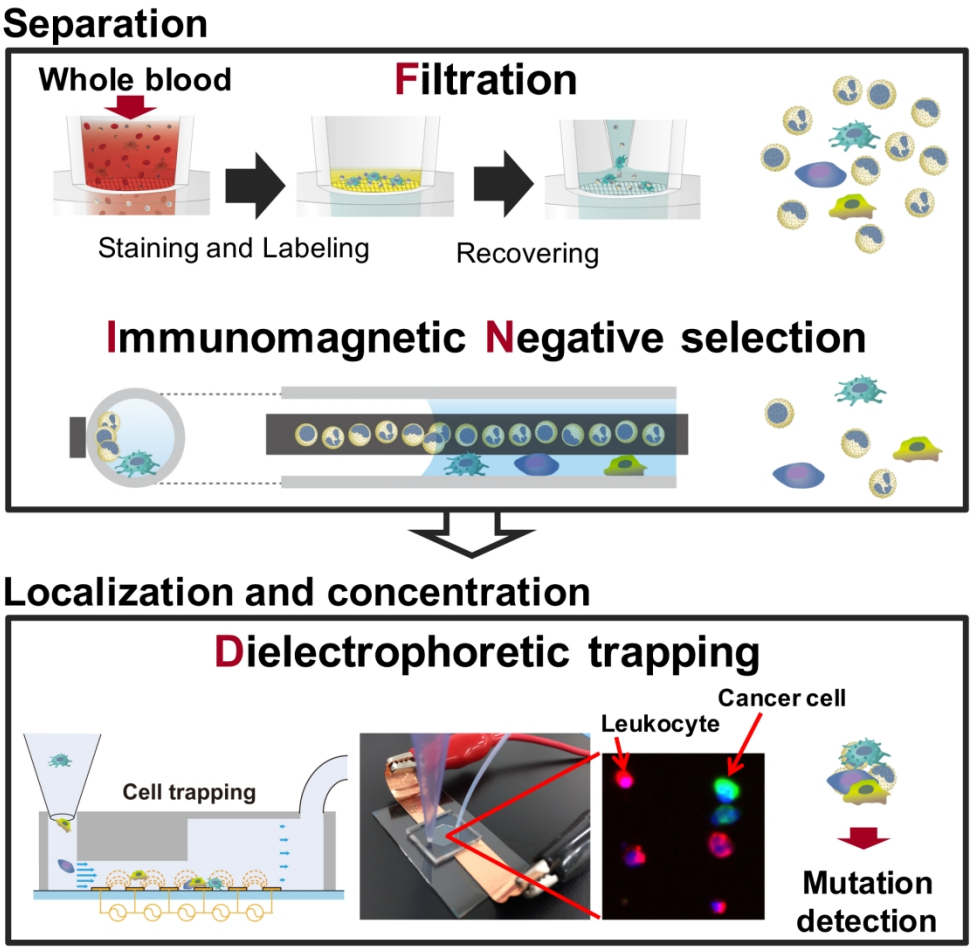

Figure 2 A schematic illustration of CTC-FIND.

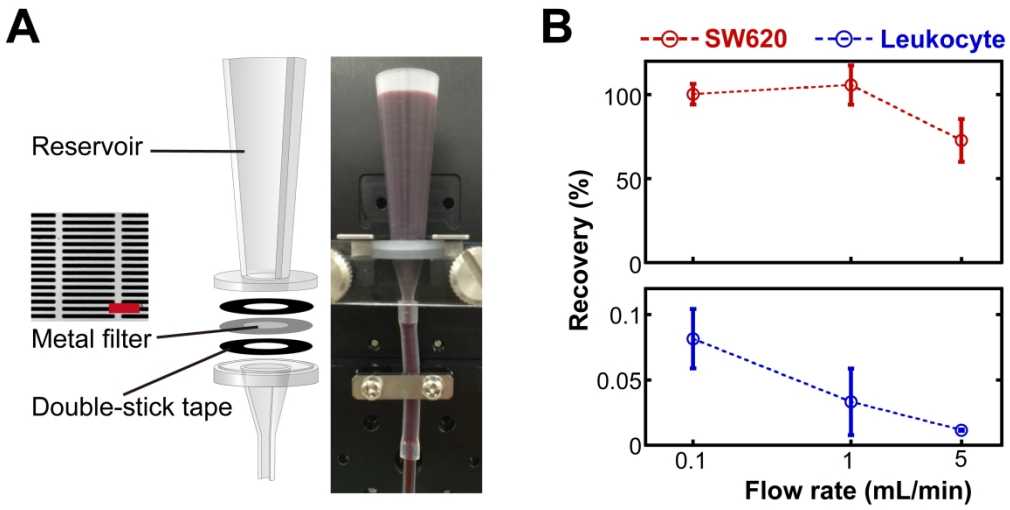

Figure 3 Size-based filtration module.

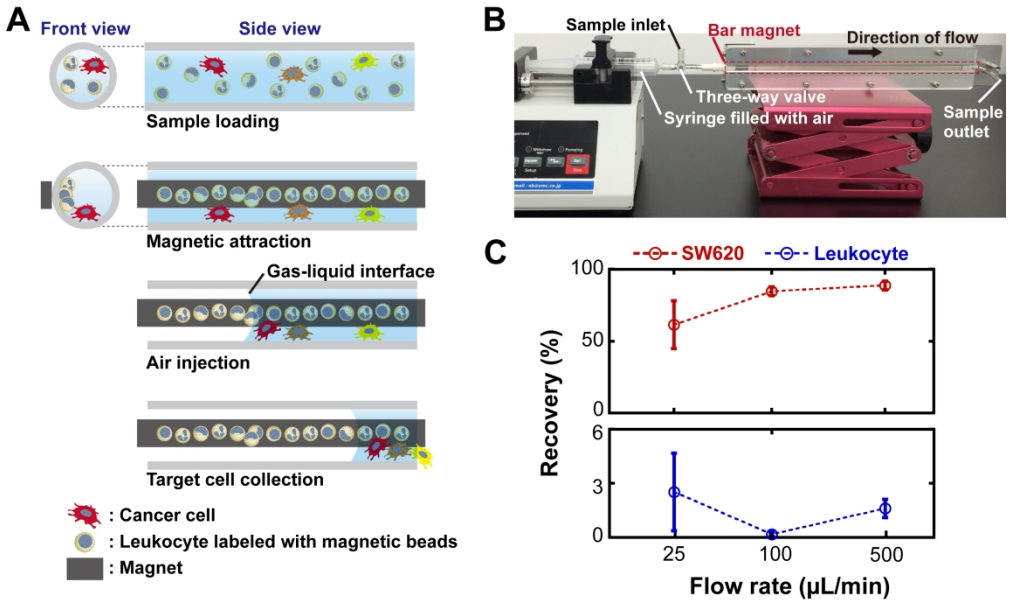

Figure 4 Immunomagnetic negative selection module.

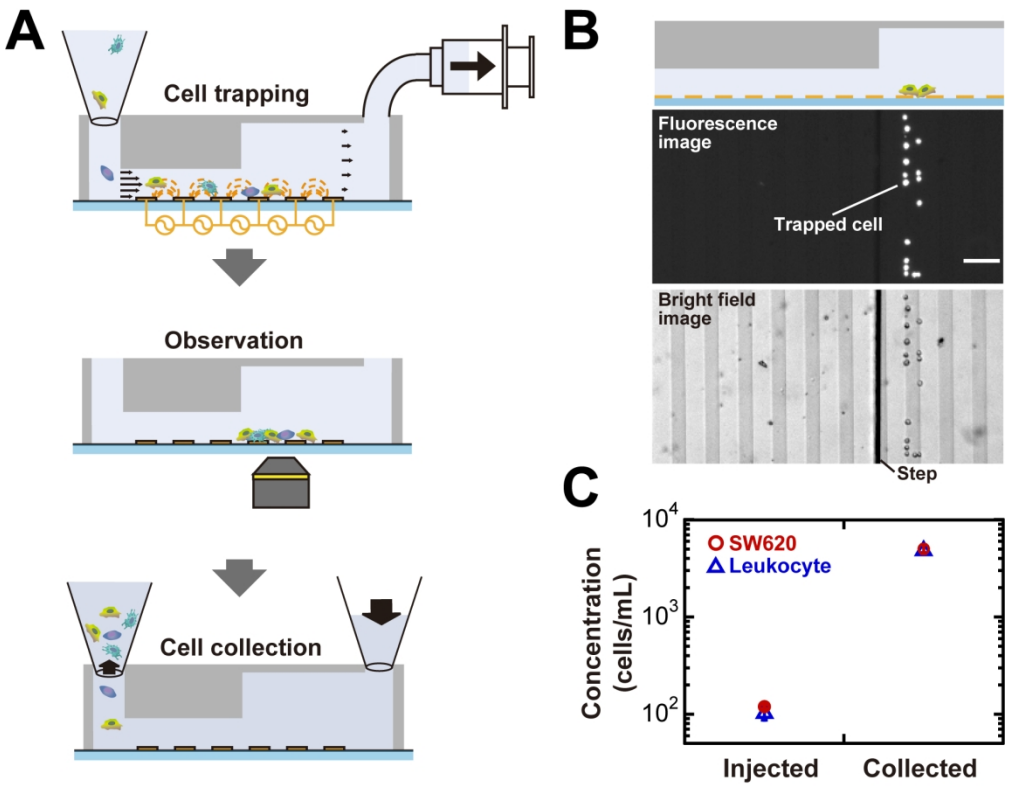

Figure 5 Localization and concentration of cells using a microfluidic step-channel.

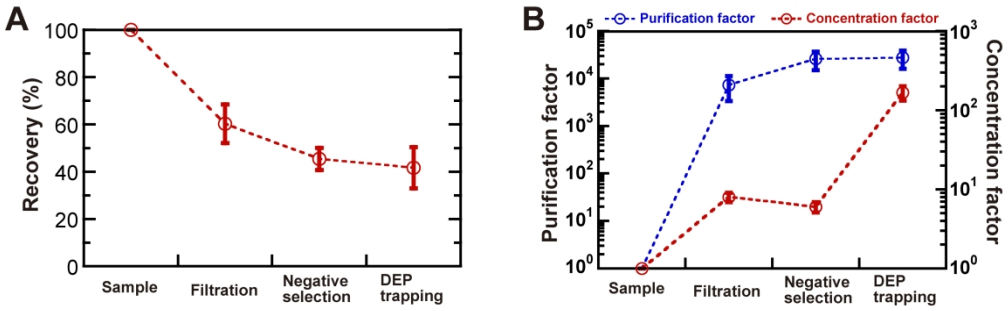

Figure 6 Changes in recovery, purification and concentration factors.